AUTHOR QUERY FORM

ELSEVIER	**Journal: OREGEO** **Article Number: 1120**	**Please e-mail or fax your responses and any corrections to:** **Moorthy, Hemalatha** **E-mail: Corrections.ESCH@elsevier.spitech.com** **Fax: +1 619 699 6721**

Dear Author,

Please check your proof carefully and mark all corrections at the appropriate place in the proof (e.g., by using on-screen annotation in the PDF file) or compile them in a separate list. Note: if you opt to annotate the file with software other than Adobe Reader then please also highlight the appropriate place in the PDF file. To ensure fast publication of your paper please return your corrections within 48 hours.

For correction or revision of any artwork, please consult http://www.elsevier.com/artworkinstructions.

Any queries or remarks that have arisen during the processing of your manuscript are listed below and highlighted by flags in the proof. Click on the 'Q' link to go to the location in the proof.

Location in article	Query / Remark: click on the Q link to go Please insert your reply or correction at the corresponding line in the proof
Q1	Please confirm that given names and surnames have been identified correctly.
Q2	"nº samples" was changed to "No. of samples". Please check if appropriate and amend if necessary.
Q3	Citation "Freyssinet, 2005" has not been found in the reference list. Please supply full details for this reference.
Q4	Highlights should consist of only 85 characters per bullet point, including spaces. However, the Highlights provided for this item exceed the maximum requirement; thus, they were not captured. Kindly provide replacement Highlights that conform to the requirement for us to proceed. For more information, please see the Guide for Authors.
Q5	Please check keywords if captured appropriately.
Q6	"Riotinto" was changed to "Rio Tinto" in all occurrences. Please check and amend if necessary.
Q7	Citation "Anthony et al., 2009" has not been found in the reference list. Please supply full details for this reference.
Q8	Citation "Seward, 1973" has not been found in the reference list. Please supply full details for this reference.
Q9	Chemical reactions (4) and (5) seem to be identical. Please check.
Q10, Q11	Please check if the insertion of a full stop here is appropriate and amend if necessary.
Q12	The citation "González, 2002" has been changed to match the author name/date in the reference list. Please check here and in subsequent occurrences, and correct if necessary.
Q13	Citation "Simancas et al., 2003" has not been found in the reference list. Please supply full details for this reference.
Q14	The citation "Simancas et al., 1983" has been changed to match the author name/date in the reference list. Please check here and in subsequent occurrences, and correct if necessary.

Q15	The word “botroidal” was changed to “botryoidal” in all occurrences. Please check and amend if necessary.
Q16	The word “respectively” was inserted here. Please check if appropriate and amend if necessary.
Q17	This sentence has been slightly modified for clarity. Please check that the meaning is still correct, and amend if necessary.
Q18	Please check the insertion of the preposition “to” here if appropriate and amend if necessary.
Q19, Q20	The phrase “shown in Eqs.” was inserted here. Please check if appropriate and amend if necessary.
Q21	Citation “Davis et al., 1996” has not been found in the reference list. Please supply full details for this reference.
Q22	Please provide an update for reference “Yesares et al., in preparation”.

Please check this box if you have no corrections to make to the PDF file. ☐

Thank you for your assistance.

Ore Geology Reviews xxx (2013) xxx–xxx

Contents lists available at ScienceDirect

Ore Geology Reviews

journal homepage: www.elsevier.com/locate/oregeorev

Supergene enrichment of precious metals by natural amalgamation in the Las Cruces weathering profile (Iberian Pyrite Belt, SW Spain)

Lola Yesares [a,*], Reinaldo Sáez [a], José Miguel Nieto [a], Gabriel Ruiz de Almodóvar [a], Stephen Cooper [b]

[a] Department of Geology, University of Huelva, Avenida de las Fuerzas Armadas, S/N, 21071 Huelva, Spain
[b] Technical Department of Cobre Las Cruces S.A., Ctra. SE-3410, Km 41,100, 41860 Gerena, Seville, Spain

ARTICLE INFO

Article history:
Received 5 February 2013
Received in revised form 16 October 2013
Accepted 17 October 2013
Available online xxxx

Keywords:
Au–Ag–Hg amalgams
Gossan
Las Cruces ore
Iberian Pyrite Belt
Au
Ag
Hg

ABSTRACT

Natural Au–Ag–Hg alloys occur in the Las Cruces ore deposit, in the eastern part of the Iberian Pyrite Belt. They are mainly concentrated in the lower part of the gossan profile including a sheared black shale level where the gossan makes contact with a barren pyrite zone within the supergene Cu-rich mineralization.

Drill core analyses show a heterogeneous distribution of Au, Ag, and Hg within the weathering profile, with mean values of 5.1 ppm, 155 ppm, and 52 ppm, respectively. In general, the absolute tenures increase towards the bottom of the weathered profile. Mineralogical studies conducted on samples from the active mine workings indicate that Hg and precious metals occur mainly as Au–Ag–Hg alloys. These associations constitute the best potential resource for precious metals at the Las Cruces deposit.

This paper describes how this unusual precious metal enrichment is produced along the weathering profile by supergene processes. Combining paragenetic information, mineral chemistry and the data pertaining to the solubilities of Au, Ag, and Hg in a weathering profile, we suggest a two-stage genetic model for the formation of the Las Cruces Au–Ag–Hg mineralization: (1) release of Au, Ag, and Hg from the massive sulfide deposit by weathering processes during the gossan formation. At pH < 5.5 and Eh > 0.9 V conditions, Au, Ag and Hg are mobilized downward through the weathering profile as chloride complexes and fixed as elemental Au, halides, oxides, and sulfates; and (2) remobilization of Hg, Ag, and Au in the gossan after the deposit was buried beneath the Neogene carbonate-rich sedimentary cover. The buffering capacity of the percolating fluids due to their interaction with the carbonate-rich sedimentary pile leads to significant mineralogical and geochemical changes. At near-neutral conditions (pH = 6–7; Eh ≈ 0 V), Hg, Ag, and Au are newly-remobilized as thiosulfate, sulfate, and hydroxide complexes and newly-fixed by sorption during ferric hydroxide formation and as sulfates. Several cycles of dissolution–precipitation of Au, Ag, and Hg near the redox front occur by oscillations in the water table and changes in the pH–Eh conditions. The interaction of downward migrating fluids with high reductant lithologies (black shales and massive sulfides) seems to be responsible for the reduction of different complexes and for the precipitation of cinnabar, Ag-sulfides and sulfosalts as well as the precipitation of Au–Ag–Hg amalgams.

1. Introduction

The Iberian Pyrite Belt (IPB) has been continuously explored and mined for more than 4500 years (Nocete et al., 2005; Sáez et al., 2003) and includes precious metals within massive sulfide weathering profiles. Examples of gossans mined for Au and Ag since prehistoric times are Rio Tinto and Filón Sur-Tharsis. Las Cruces is a recently discovered volcanic-hosted massive sulfide deposit in the IPB whose supergene profile differs from known others and contains large resources of precious metals.

Supergene precious metal ores occur essentially as the result of concentration during the weathering of hypogene deposits. In near-surface environments, Ag and Au are released during the oxidative dissolution of primary sulfides. These metals are concentrated and redistributed through the oxidation profile by residual concentration processes.

The mobilization and enrichment of precious metals in oxidizing and acidic environments are well documented (Benedetti and Bouleguè, 1991; Boyle, 1979; Freyssinet et al., 2005; Hough et al., 2009; Reich et al., 2005; Webster and Mann, 1984). Under extreme conditions, precious metals are mobilized through the weathering profile via complexation by different anions, such as a CN^{2-}, OH^-, NH_3, Cl^-, I^-, Br, and HS^- (Groen et al., 1990) until reaching an environment with physical–chemical conditions favorable for precipitation.

Under oxidizing conditions, native Au is the only specie stable (Krupp and Weiser, 1992), whereas Ag can occur as a native element, as halides such as chlorargyrite [ClAg], iodargyrite [IAg], and bromargyrite [BrAg]; or as sulfates of the jarosite group (i.e., argentojarosite [$AgFe_3(SO_4)_2(OH)_6$]) (Dutrizac and Jambor, 1987).

Regarding the supergene profiles of the IPB, native Au has been reported in Filón Sur-Tharsis (Capitán, 2006) and Rio Tinto (Viñals et al.,

* Corresponding author.
E-mail address: lola.yesares@dgeo.uhu.es (L. Yesares).

0169-1368/$ – see front matter © 2013 Published by Elsevier B.V.
http://dx.doi.org/10.1016/j.oregeorev.2013.10.004

1995) and the main Ag-bearing phases are halides, acanthite, and argentojarosite, in both Rio Tinto (Capitán, 2006; Viñals et al., 1995) and Tharsis (Capitán, 2006). The burial of the Las Cruces deposit after oxidation resulted in significant changes that make it very different to common models of precious metal concentration during gossan formation. The most important concerns the formation of Au–Ag–Hg amalgams as the main precious metal minerals at Las Cruces. Hg–Ag amalgams have also been reported in the Lagoa Salgada gossan (Oliveira et al., 2011), whose supergene evolution is similar to that of the Las Cruces deposit. The occurrence of Au–Ag amalgams has consequences regarding the mechanisms of mobilization and precipitation of precious metals in supergene environments.

2. Au, Ag, and Hg mobilization and fixation in supergene profiles

The physico-chemical conditions of precious metal redistribution in weathering profiles have been well documented (Benedetti and Bouleguè, 1991; Krupp and Weiser, 1992; Mann, 1984; Webster and Mann, 1984). Different mechanisms for Au and Ag dissolution, mobilization, and precipitation have been proposed. In oxygenated aqueous solutions, Au and Ag are soluble and transported by organic complexes (Boyle et al., 1975), halogen complexes (Mann, 1984), hydroxide complexes (Wood, 1990), and sulfur ligand complexes (Webster, 1986).

Supergenic redistribution of Au and Ag through the weathering profile is dependent on the nature and stability of anionic complexes and their behavior under near-surface weathering conditions (Webster and Mann, 1984). Au and Ag released from the oxidation of primary sulfides are slightly mobilized when the environmental conditions are extremely acidic. These species can be transported down short distances along the weathering profile to environments where the conditions are less acidic. Mann (1984) proposed that in an acidic, oxygenated, saline and Fe-rich aqueous stream environments (pH < 5.5; Eh > 0.9 V; activity $Cl^- > 10^{-3.2}$), precious metals are mobilized through the weathering profile as Au– and Ag–chloride complexes (Webster and Mann, 1984). These conditions are common in oxidized meteoric waters containing abundant chlorine derived from the dissolution of salts (Ross, 1997). The dissolution of Au and Ag to form chloride complexes is expressed by the following chemical reactions:

$$4Au + 16Cl^- + 3O_2 + 12H^+ = 4AuCl_4^- + 6H_2O \text{(Mann, 1984)} \quad (1)$$

$$4Ag + 4Cl^- + O_2 + 4H^+ = 4AgCl^0 + 2H_20 \text{(Mann, 1984)}. \quad (2)$$

Au precipitation can be produced by inorganic reduction of Au-chlorides by a slight decrease in Eh (Hough et al., 2008), and also by the reduction of the $AuCl_4^-$ ion with Fe^{2+} by the reaction:

$$4AuCl_4^- + 3Fe^{2+} + 6H_2O = Au^0 + 3FeOOH + 4Cl^- + 9H^+ \text{(Mann, 1984)}. \quad (3)$$

This reaction involves the simultaneous deposition of both native Au and iron hydroxide. However, $AgCl^0$ is not precipitated as native Ag by the oxidation of Fe^{2+} because the redox potential for $Ag^0/AgCl^0$ is below that of the Fe^{2+}/Fe^{3+} couple (Mann, 1984). Therefore, $AgCl^0$ remains in solution, migrating downward (Saunders, 1993) until reaching an environment where the physico-chemical conditions are less extreme, allowing its precipitation as chlorargyrite.

The sulfide breakdown during weathering processes releases a number of metastable sulfur species as SH^-, $S_2O_3^{2-}$, SO_3^{2-} and SO_4^{2-} (Freyssinet et al., 2005). All of them can favor precious metal transport through the profile and can be transformed according to pH and oxygen fugacity (Krupp and Weiser, 1992). Au bisulfide complex $[Au(SH)_2^-]$ can occur in supergene environments under reducing conditions (Anthony et al., 2009; Webster, 1986) and pH near to neutral (Vlassopoulos and Wood, 1990), for example during early supergene alteration stages (Gray et al., 1992). Hence, SH^- ligand is not so important in supergene environments (Freyssinet et al., 2005) although it can be particularly significant in hydrothermal systems (Boyle, 1979; Seward, 1973).

At near-neutral conditions (pH = 6–7; Eh ≈ 0 V) and in the presence of weathered carbonate rocks, the formation of thiosulfate and/or sulfite ions during sulfide oxidation favors the migration of Au and Ag along the weathering profiles as $Au–Ag(S_2O_3)_2^{3-}$ and $Au–Ag(SO_3)_2^{3-}$ (Benedetti and Bouleguè, 1991; Boyle, 1979; Webster and Mann, 1984). Due to its slow kinetic transformation (Rolla and Chakrabarti, 1982), thiosulfate could remain in solution over relatively long periods. Thus, thiosulfate is the most probable complex under near-surface environment and neutral conditions (Webster and Mann, 1984).

The dissolution of Au and Ag to form thiosulfate complexes is expressed by the chemical reactions:

$$2Au^0 + 4S_2O_3^{2-} + H^+ + 0.5O_2 = 2Au(SO_3)_2^{3-} + H_2O \text{(Freyssinet et al., 2005)} \quad (4)$$

$$2Ag^0 + 4S_2O_3^{2-} + H^+ + 0.5O_2 = 2Ag(SO_3)_2^{3-} + H_2O. \quad (5)$$

In addition, the precious metal mobilization as thiosulfate complexes have been successfully used to Au and Ag industrial extraction and recovery of different ore types (Aylmore and Muir, 2001).

However, if the redox conditions increase, thiosulfates are readily oxidized and converted to sulfates (Benedetti and Bouleguè, 1991; Freyssinet et al., 2005). Au—sulfate complexes would rapidly decompose, leaving Au as an uncomplexed Au^+ ion, which would be precipitated by reduction to Au^0 as submicroscopic particles (Benedetti and Bouleguè, 1991) or within the mineralized structures (Freyssinet et al., 2005).

The Au precipitation can be expressed by the following chemical reaction:

$$Au^+ + Fe^{2+} + 2H_20 = Au^0 + FeOOH + 3H^+ \text{(Stroffregen, 1986)}. \quad (6)$$

Moreover, Ag sulfate remains as stable species in solution (Krupp and Weiser, 1992). The high solubility of Ag_2SO_4 makes its occurrence as a stable oxidation product of Ag unlikely, although more complex sulfate phases (i.e., argentojarosite) are common in sulfide weathering profiles (Dutrizac and Jambor, 1987). Hence, Ag_2SO_4 is transported through the oxidation profile to the water table, where Ag_2SO_4 becomes destabilized through reduction and Ag can be reprecipitated as sulfide below the redox front.

Hg mobilization during the massive sulfide weathering is less well documented. Therefore, little is known about the mechanisms of Hg dissolution and re-precipitation in these environments.

During sulfide weathering, mercurous compounds (Hg^+) are rapidly oxidized to mercuric forms (Hg^{2+}) and are slightly mobilized through the weathering profiles as $HgCl_2^0$, which is the stable species in solution under oxidizing and acidic conditions (Davis et al., 1997). The oxidative dissolution of Hg to form chloride complexes could occur through the reaction:

$$Hg^{2+} + 2Cl^- + 3O_2 + 12H^+ = HgCl_2^0 + 6H_2O. \quad (7)$$

Under neutral and high pH conditions, Hg^{2+} is stable in solution and is easily complexed by OH^-, enhancing its solubility by the reactions:

$$Hg^{2+} + 0.5O_2 + H_2O = Hg(OH)_2^0 + H^+ \quad (8)$$

$$HgCl_2 + 2H_2O = Hg(OH)_2^0 + 2H^+ + Cl^- \text{(Hepler and Olofsson, 1975)}. \quad (9)$$

The redistribution and fixation of secondary Hg-minerals through the weathering profile are dependent on the redox and pH conditions. Under oxidizing and acidic conditions, Hg^{2+} can be precipitated as

Please cite this article as: Yesares, L., et al., Supergene enrichment of precious metals by natural amalgamation in the Las Cruces weathering profile (Iberian Pyrite Belt, SW Spain), Ore Geol. Rev. (2013), http://dx.doi.org/10.1016/j.oregeorev.2013.10.004

montroydite (HgO), calomel (Hg_2Cl_2), and sulfate minerals of the jarosite group (Dutrizac and Eno, 1981) through the following chemical reactions:

$$2HgCl_2^0 + 2Cl^- = Hg_2Cl_2 + Cl_2 \quad (10)$$

$$HgCl_2^0 + H_2O = HgO + 2Cl^- + 2H^+ \quad (11)$$

$$0.5Hg^{2+} + 3Fe^{3+} + 2SO_4^{2-} + 6H_2O = Hg_{0.5}Fe_3(SO_4)_2(OH)_6 + 6H^+ \text{(Dutrizac and Eno, 1981)}. \quad (12)$$

In contrast, under neutral conditions, Hg^{2+} can be sorbed to ferric hydroxides up to pH 8 as $Hg(OH)^0_2$ (Davis et al., 1997). Furthermore, in Fe-rich environments, Fe^{2+} can act as a reductant, and its oxidation could conceivably couple to Hg^{2+} reduction. This process can be initiated by reactions with Fe^{2+} at mineral surfaces, resulting in the dissolution and release of Hg into the environment (Charlet et al., 2002) by the reaction:

$$Hg(OH)_2 + Fe^{2+} = Fe(OH)_3 + Hg^0 \text{(Charlet et al., 2002)}. \quad (13)$$

This reaction implies a simultaneous deposition of both iron oxyhydroxides and Hg.

3. Geological setting

The Las Cruces VHMS deposit is located in the eastern part of the IPB. The deposit is covered by a thick sequence (140–150 m) of detrital and carbonated rocks belonging to the post-Alpine (Neogene–Quaternary) Guadalquivir River foreland basin (Fig. 1). The IPB is the largest domain of the South Portuguese Zone, the southernmost domain of the Iberian Variscan Massif (Julivert et al., 1974), and among the most prolific massive sulfide provinces in the world (Leistel et al., 1998; Sáez et al., 1999). Its stratigraphic record, Middle Devonian–Mississippian in age, is characterized by intense bimodal magmatic activity and an abundance of enormous massive sulfide deposits. From footwall to hanging wall, it has been classically subdivided into three main units: the Givetian–Famennian Pre-Volcanic Phyllite–Quartzite Group, the Late-Famennian–Tournaisian Volcano-Sedimentary Complex, and the Visean–Westphalian B Post-Volcanic Culm Group (Schermerhorn, 1971). The massive sulfide deposits of the IPB are included in the Volcano-Sedimentary Complex, always associated with felsic–volcaniclastic and/or black shale sequences. Geochronologic data have constrained the age of massive sulfide deposition to the Late Devonian–Mississippian (Barrie, 2002; Nesbit et al., 1999; Nieto et al., 2000). Palynological data obtained from hosting black shale of the main ore deposits suggest a massive sulfide event linked to the Devonian–Carboniferous boundary (González et al., 2002; González et al., 2006; Sáez et al., 2008). During the Pennsylvanian, the inversion of the tectonic regime from transtensional to compressional (Simancas et al., 2003) resulted in the deformation and the very low-grade metamorphism of the IPB rocks according to a thin-skinned tectonic model (Silva et al., 1990). As a result of the deformation, the exhumation of the Variscan chain exposed the massive sulfide deposits to the surface, thus promoting oxidation and the formation of gossans. Later, the Neogene transgression led to the burial of a part of the IPB under the post-Alpine sediments of the Guadalquivir and Sado river basins. Las Cruces and Lagoa Salgada represent cases of recently discovered massive sulfide deposits, hidden below the Neogene–Quaternary sedimentary cover.

4. Ore deposit

The Las Cruces deposit is located approximately 24 km NW of Seville (Spain). The mining project is currently operated by Cobre Las Cruces, a local subsidiary of the Immet Mining Corporation and Leucadia National Corporation. The present project involves the open pit mining and hydrometallurgical processing of 17.6 Mt of 6.2% Cu ore in a leaching plant close to the mine site. The current 12-year mining plan estimates the production of approximately 1 Mt of high-grade copper with a mean recovery of 92% of ore Cu content. In addition, there is approximately 2 Mt of gossan with significant contents of Au, Ag, and Pb.

The Las Cruces deposit consists of an approximately 100-m-thick massive sulfide body. It is hosted in a thick sequence of black shales, including felsic–volcanic and volcaniclastic rocks (Fig. 2A, B). The orebody extends over more than 1 km in the E–W direction, dipping to the north at approximately 35° (Fig. 2A), and is composed of a polymetallic massive sulfide body underlain by cupriferous and pyritic stockwork type mineralization. The upper part of the massive sulfide consists of a supergene profile that includes a copper-rich cementation zone, which constitutes the ore, and the upper gossan (Figs. 2A, 3A).

Several structural domains have been observed in the Las Cruces ore, which are in agreement with the tectonic style established for the IPB by Silva et al. (1990). The first fault system comprises subhorizontal trending faults, associated with the first Variscan deformation phase in the IPB (Fig. 3A). These low-angle fault systems were responsible for the overthrusting of different massive sulfide slices often being detached along the black shale hosting horizons. Examples of this structural framework have been described in the Tharsis (Tornos et al., 1998), Aznalcóllar (Almodóvar et al., 1998), Sotiel-Coronada (González et al., 2006), and Neves Corvo (Relvas et al., 2002) mine districts. At the Las Cruces deposit, this phenomenon is responsible for several massive sulfide sheets being stacked and limited by the sheared

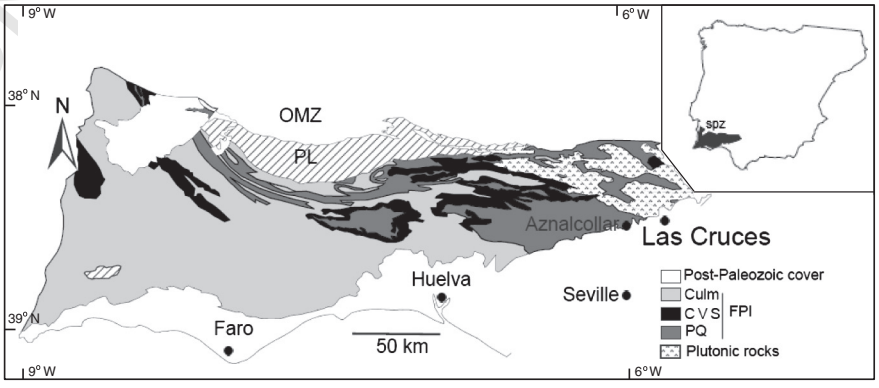

Fig. 1. Geological map of the Iberian Pyrite Belt (modified from Carvalho, 1976), indicating the location of the Las Cruces deposit. Geological abbreviations: IPB, Iberian Pyrite Belt; OMZ, Ossa Morena Zone; PL, Pulo do Lobo Terrane.

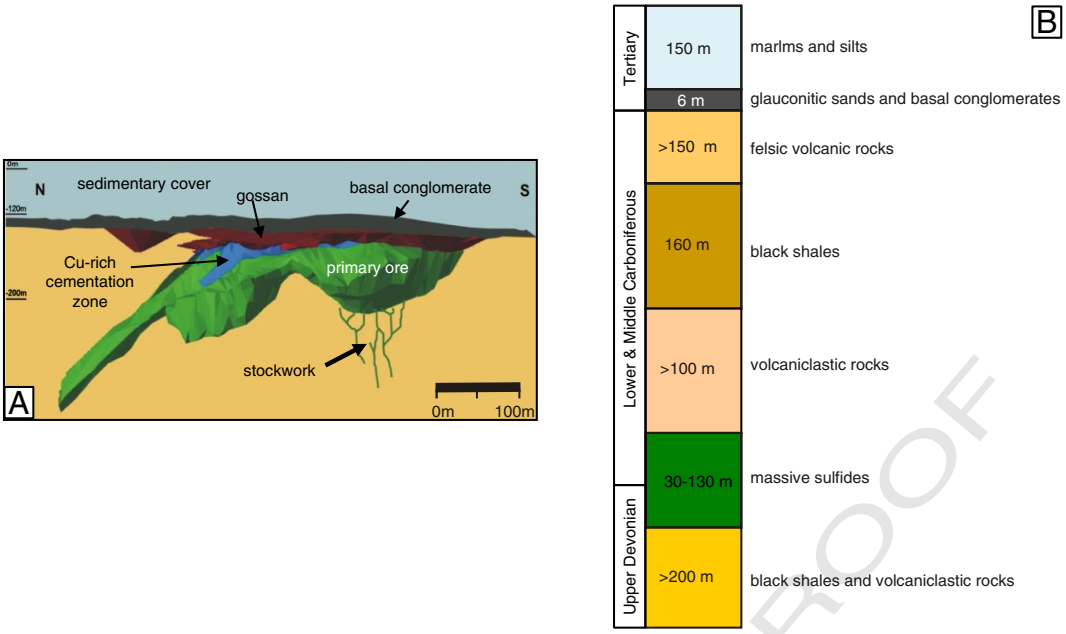

Fig. 2. (A) Geological sketch section; and (B) stratigraphic column of the Las Cruces deposit showing the different ore-types, the host rock sequence, and the sedimentary cover.

black shale sheets (Fig. 3B, C, D). The second and third fault systems comprise subvertical faults (Fig. 3A), which have been related to late-Variscan deformation (Simancas, 1983). The older system consists of NNW/SSE trending faults, which control the secondary mineralization processes. Faults belonging to this system, as well as the ore deposit, are intersected by a younger system represented by E–W high-angle faults.

The primary ore at the Las Cruces deposits exhibits mineralogical features similar to other massive sulfide deposits in the IPB (Marcoux et al., 1996) and is mainly composed of pyrite and small amounts of sphalerite, chalcopyrite, and galena. Tetrahedrite–tennantite, arsenopyrite, and different Bi- and Pb-sulfosalts are common accessory minerals. This ore is very irregular in shape and mineralogy, including barren pyrite, polymetallic-rich and copper-rich facies.

The thickness of the overlying gossan ranges from 0 to 20 m. It is limited at the bottom by a sharp horizontal contact with the massive sulfides and at the top by an erosive discordant contact with the sedimentary cover (Fig. 3A). The occurrence of gossan pebbles within

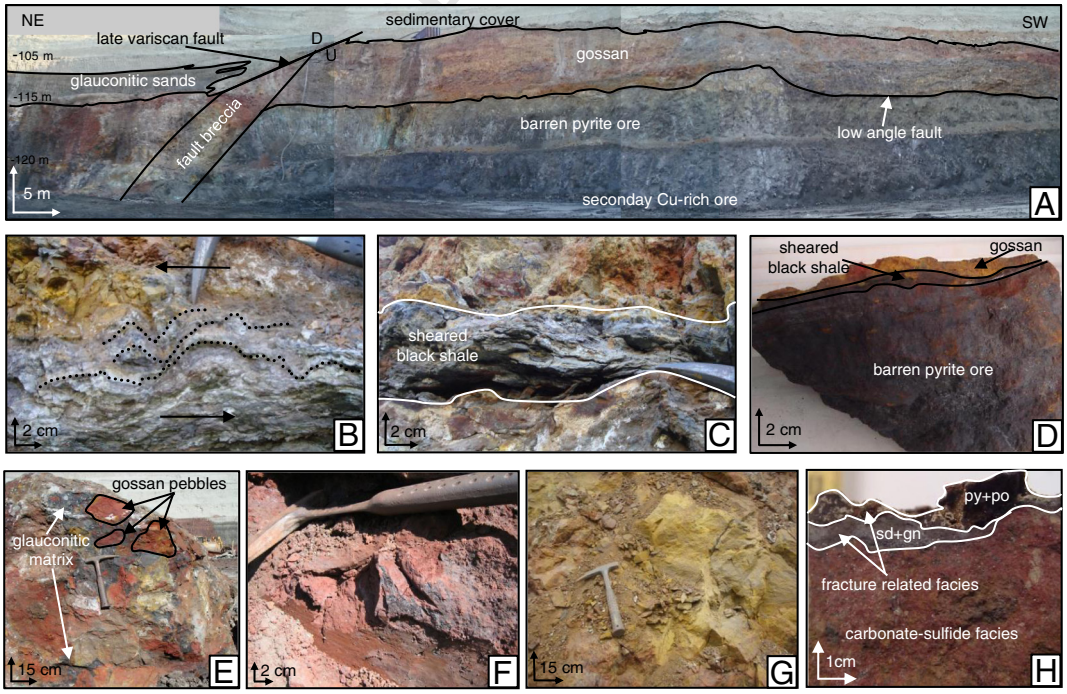

Fig. 3. Las Cruces outcrops overview. (A) NE–SW section of the open pit first stage showing the contact of the gossan with the primary ore (below) and with the sedimentary cover (above); (B) and (C): sheared black shale level. Drag folds indicating the direction of movement can be observed (D); (E) basal conglomerate: gossan pebbles in a glauconitic sand matrix; gossan facies: (F) Fe-oxide facies; (G) carbonate-sulfide facies; and (H) fracture-related facies.

Please cite this article as: Yesares, L., et al., Supergene enrichment of precious metals by natural amalgamation in the Las Cruces weathering profile (Iberian Pyrite Belt, SW Spain), Ore Geol. Rev. (2013), http://dx.doi.org/10.1016/j.oregeorev.2013.10.004

the basal conglomerate of the sedimentary cover (Fig. 3E) indicates that the weathering and oxidation of the massive sulfide predate the transgressive Neogene deposits. Regional biostratigraphic and geochronologic data on this sedimentary cover establish a Tortonian minimum age for gossan burial (Moreno et al., 2002), this data being consistent with the age proposed for the major period of IPB gossan formation (Essalhi et al., 2011; Velasco et al., 2013).

The Las Cruces gossan differs from other weathering profiles by (1) an uneven mineral association; and (2) its high mineralogical and geochemical heterogeneity both vertically and laterally as well as the absence of internal structure, which is common elsewhere for sulfide alteration profiles (Jambor et al., 2000; Scott et al., 2001) included IPB gossans (Capitán, 2006; Capitán et al., 2003). Unlike other gossans, which are mainly composed of oxidized phases (i.e., Fe-oxides and Fe-sulfates), the mineral composition of the Las Cruces gossan is dominated by iron reduced phases, including siderite and pyrite, whereas oxidized phases are subordinated. Calcite and galena are also major mineral components.

Despite the lack of internal structure within the Las Cruces gossan, its mineralogical and textural features define several facies:

- Carbonate-sulfide facies: This category constitutes the main facies of the gossan and is distributed heterogeneously through the profile (Fig. 3F). It is composed mostly of massive siderite and minor hematite, goethite, galena, and Fe-sulfides, including pyrite, marcasite, pyrrhotite and greigite. In addition, subordinate amount of Ag-sulfides and Au–Ag–Hg amalgams can be observed. These facies are characterized by dissolution–replacement textures in which massive siderite replace former Fe-oxyhydroxides (i.e., hematite and goethite).
- Fe-oxide facies: Although pervasive in the gossan, the facies is usually located close to highly porous zones. It is mainly composed of goethite and hematite, with siderite, Fe-sulfides, and galena as subordinated minerals. Different textural patterns characterize Fe-oxyhydroxides, including (1) primarily gossan relicts cemented by siderite, (2) alternating botryoidal siderite and oxyhydroxide microlayers, and (3) poorly developed colloforms resulting from the oxidation of siderite (Fig. 3G).

The relationships between the facies are not evident. However, some roughly vertical alternating pattern can be identified in the profile (Fig. 3A).

- Fracture-related facies: This category consists of coarse grained siderite, galena, and Fe-sulfides, which occur as euhedral equigranular aggregates filling voids associated with late fractures that cut the whole profile (Fig. 3H).
- Leached black shales: The contact between a decomposed barren pyrite zone, located at the top of the secondary Cu-rich ore, and gossan is marked by a 5-to-15-cm-thick black shale horizon. (Fig. 3 A, B, C, D). Open pit exposure suggests this contact to be controlled by a low-angle Variscan fault and the black shale horizon, acting as a detachment level during fault development. Due to the strong leaching, primary features in these rocks such as fissility, particle size and composition are poorly preserved. The assignment as sheared black shales is supported by its PAAS normalized geochemical profile (Yesares et al., in preparation). This shows a typical geochemical black shale pattern but enriched in immobile elements such as Si, Al, Ti, Zr, Y, Sn, U, Th, W, and REE.

Leached black shales are mainly composed by residual minerals such as quartz, barite, monazite, and Ti-oxides. Moreover, the newly-formed mineralogy predominantly consists of supergene minerals as phyllosilicates of the smectite and kaolinite groups. In addition, fine-grained galena occurs as skeletal aggregates and Ag-sulfides, cinnabar and Au–Ag–Hg amalgams are common as filling voids. The barren pyrite within the supergene Cu-rich mineralization is located at the footwall of the black shale level.

Other lithologies have been described in the Las Cruces gossan on the basis of drill core lithochemical studies. For example, Knigth (2000) reported a "silica cap" between the gossan and the secondary massive sulfides. The silica cap is highly variable in thickness. It consists of fine grained silica clasts, siliceous cement and subordinate amounts of iron oxides and clays. This lithology has been identified in the open pit outcrops but their distributions are meagre.

The underlying massive sulfide includes a thick cementation zone, characterized by secondary Cu-sulfides such as chalcocite, digenite, djurleite, covellite, enargite, and bornite (Yesares et al., 2012). Ore distribution both in the gossan and Cu-rich cementation zones seems to be controlled by late-Variscan tectonic structures reactivated during the Alpine tectonic cycle (Yesares et al., 2012) (Fig. 3A).

5. Samples and analytical procedures

The most relevant geological, lithological, and structural observations and interpretations have been made during the construction of the open pit. The selected samples, mainly of gossan and other ore types were collected during the first and second mining stage of the open pit. In addition, some key samples have been obtained from drill cores.

In all, 231 polished sections were made for mineralogical and textural studies with optical and scanning electronic microscopes. Among them, 21 sections were used for detailed studies of Au–Ag–Hg. Amalgam characterizations were conducted after small surface analysis with a JEOL scanning electron microscope coupled with energy dispersive spectroscopy (SEM–EDS). Forty successful SEM analyses of amalgams were obtained. The mineral chemistry of Au–Ag–Hg amalgams was investigated by electron-microprobe analysis using a JEOL JXA-8200 Super Probe Electron Probe Micro-Analyzer (EPMA). Possible crystal zoning has also been checked. Concentrations of Ag, Au, and Hg were determined by wavelength-dispersive spectroscopy (WDS) equipment. In all, 57 successful EPMA analyses of amalgams have been obtained. Due to difficulties related to the high volatility of Hg, special operating conditions were employed. The main operating parameters were 10 kV, 10 nA, and 5–8 μm. Pure Au and Ag and synthetic HgS (Au Mα, Ag Lα, and Hg Mα) were used as standards. Routine data reductions, including full matrix (ZAF) corrections, were performed. No corrections were made for potential "loss" of Hg during analysis. However, the migration of Hg in response to heating by the electron beam is believed to be systematic, as the analytical conditions and counting times were kept identical for the unknowns and the well-characterized standards. To prevent loss of Hg by evaporation during EPMA analyses, trace elements were not included in the analytical routine. However, the SEM–EDS analyses of amalgams show the consistent presence of Ag, Au and Hg in varying proportions, whereas trace elements occur in undetectable amounts.

Geochemical modeling of the precious metals and Hg has been undertaken after the statistical treatment of the Las Cruces database. This database includes geochemical analyses of cores from 305 drill holes performed during the exploration and evaluation stages. Ag, Au and Hg were measured in 8348 select samples from gossan, Cu-rich cementation zone, primary sulfides and host rocks. The chemical assays were undertaken in several full-accredited laboratories. A first set of samples (drill hole numbers CR001-CR256) was measured by Anamet Services (Avonmouth, UK), a second set of analysis (drill hole numbers CR257-CR301) by OMAC Laboratories (Ireland), and a third set by AGQ Labs (Seville, Spain). All analyses have been conducted by the same methodology. Ag and Hg were determined after 4 acids digestion (HF, HNO_3, HCl and $HClO_4$) with inductively coupled plasma-optical emission spectrometry (ICP-OES). The concentrations of Au in the select samples were performed by Ni fire assay followed by atomic absorption spectroscopy (AAS).

Please cite this article as: Yesares, L., et al., Supergene enrichment of precious metals by natural amalgamation in the Las Cruces weathering profile (Iberian Pyrite Belt, SW Spain), Ore Geol. Rev. (2013), http://dx.doi.org/10.1016/j.oregeorev.2013.10.004

6. Results

6.1. Distribution of Au–Ag–Hg-bearing minerals

Exploration data regarding the geochemical features of the Las Cruces deposits suggest an association between the precious metals and Hg in the gossan. Drill core geochemical data, provided by Cobre Las Cruces, indicate a heterogeneous distribution of precious metals within the ore deposit. Representative values are included in Table 1. In primary sulfides, Ag and Hg are mainly associated with the polymetallic ore. Ag shows mean concentrations of 42.40 ppm, with values up to 715 ppm. Hg reaches a maximum value of 815 ppm and a mean concentration of 52 ppm. Au is also mostly associated with the polymetallic ore although minor amounts have been identified in Cu-rich ores. Au content in polymetallic ores ranges between 0.02 ppm and 8.4 ppm, showing mean values of 0.7 ppm. The Cu-rich ore exhibit Au mean of 0.5 ppm ranging from 0.1 ppm to 1.65 ppm.

Ag, Hg and Au distributions show a strong heterogeneity within the supergene profile. The cementation zone exhibits mean values of 26.7 ppm Ag, 25 ppm Hg and 0.6 ppm Au, with individual values up to 1470 ppm Ag, 11085 ppm Hg and 285 ppm Au. The whole gossan appears enriched in Ag, Hg and Au relative to primary sulfides. Although the distribution of metal values is quite heterogeneous, rough zonation is observed in the gossan profile. Mean concentrations in the upper part are 63.35 ppm Ag, 32.30 ppm Hg and 2.90 ppm Au. These values increase significantly in the lower part of the gossan reaching maximum values of 18,950 ppm, 10,500 ppm and 352 ppm respectively and showing mean concentrations of 565 ppm Ag, 615 ppm Hg and 17.20 ppm Au (Fig. 4). The main precious metal concentrations occur associated either with the carbonate-sulfide facies close to the contact between gossan and the cementation zone, or with the sheared black shale level which makes the limit between barren pyrite zone and the secondary Cu-rich mineralization and gossan.

Two principal mineral associations are observed in the carbonate-sulfide facies: (I) The most frequent mineral association comprises of siderite, calcite, Fe-sulfides and galena (Fig. 5A, B). In the lower part of the gossan profile, this facies also contains precious metal-bearing phases such as acanthite, proustite, pyrargyrite, freibergite, miargyrite, argentopyrite, sternbergite and Au–Ag–Hg amalgams. Common textures include: microcrystalline, euhedral–anhedral aggregates, skeletal aggregates, veinlets, filling fractures and voids, and intergrowths and overgrowths. Fracture and open space filling occur mainly in the lower part of the weathering profile. The commonest textures of the Ag-sulfides consist of: intergrowths and overgrowths between Ag-sulfides and pyrite; coarse grain euhedral aggregates of Ag-sulfides; and Ag-sulfide rims along pyrite edges (Fig. 6A). Au–Ag–Hg amalgams appear as finely disseminated skeletal aggregates, filling open spaces, and overgrowth with sulfides (Fig. 6A and B); and (II) Corroded fragments of Fe-rich oxides and oxyhydroxides. These are common as isolated fragments enclosed in later microcrystalline siderite (Fig. 5C) or as alternating microlayers (Fig. 5D). In addition, this association can show textures as: botryoidal, microcrystalline, and euhedral aggregates. Fragments of Fe-oxide are scarce but occur elsewhere along the gossan profile.

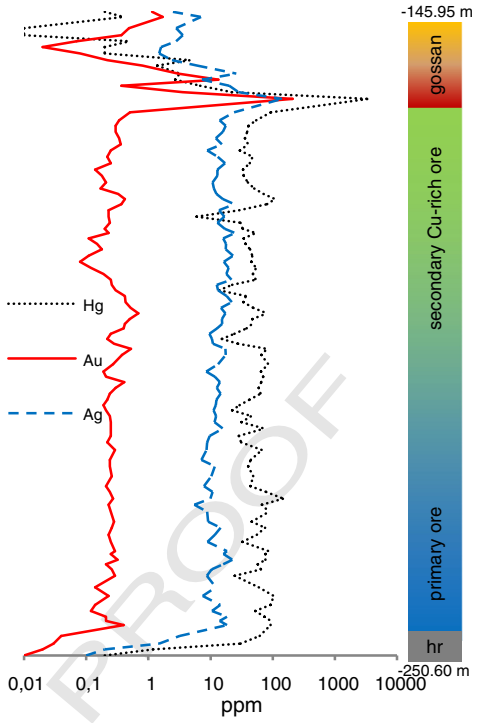

Fig. 4. Au, Ag, and Hg vertical distribution of Las Cruces deposits based on analysis from a representative drill hole crosscutting the gossan, secondary Cu-rich ore, and primary sulfides.

In the leached black shale level, the main mineral association is composed of newly-formed kaolinite and smectite along with abundant weathering-resistant minerals such as quartz, Nd–Ce–monazite, rutile and zircon. Remnants of primary sulfides, mainly pyrite, occur towards the bottom of the black shale level (Fig. 6C, D, E). The black shale-hosted Au–Ag–Hg-bearing assemblage is comprised of: proustite, pyrargyrite, imiterite, freibergite, argentopyrite, sternbergite, cinnabar, and Au–Ag–Hg amalgams. This assemblage fills open spaces within the black shale. Common textural features include: anhedral aggregates, veinlets, and intergrowths and overgrowths between Ag-sulfides and cinnabar. Au–Ag–Hg amalgams appear as coarsely disseminated grains arranged parallel to the main foliation in the black shales (Fig. 6C, D, E, F). In addition, late pyrite and galena can also be found as fine veins cross-cutting the previously described mineral association (Fig. 6C, D, F). In addition, Blake (2008) also reported rare fine grained (<5 μm) euhedral to subhedral native Au grains included in the limonite-rich gossan. They are closely associated with siderite and limonite or linked to Cu–Fe-sulfides, native Bi, Fe-sulfides, bismuthinite and Pb-sulfide. However, this Au-bearing assemblage has not been observed in the present study.

6.2. Mineralogical characterizations of Au–Ag–Hg amalgams

Reflected light microscopy, SEM–EDS, and EPMA–WDS have been used to identify the amalgams found in the lower part of the gossan.

Table 1
Au, Ag, and Hg grades of main ore types in the Las Cruces deposit.

Element (ppm)			Au			Ag			Hg		
		No. samples	Range	Mean	Median	Range	Mean	Median	Range	Mean	Median
Primary ore	Pyritic	165	0.07–0.70	0.30	0.20	3.80–35	12.00	12.00	1.30–64	18.00	15.50
	Polymetallic	2055	0.02–8.40	0. 70	0.50	0.40–715	42.40	32.50	0.30–815	52.00	43.50
	Cu-rich	539	0.10–1.65	0.50	0.45	0.20–295	28.40	18.50	0.01–140	26.00	21.50
Supergene	Cu-enrichment	4852	0.02–285	0.60	0.35	0.1–1470	26.70	15.50	0.04–11085	25.00	4.00
Gossan	Upper gossan	586	0.10–55.40	2.90	1.50	0.1–4810	63.35	19.00	0.1–7.5	32.30	32.30
	Lower gossan	151	0.50–352	17.20	8.00	0.1–18950	565	181	0.1–10500	615	53.00

Please cite this article as: Yesares, L., et al., Supergene enrichment of precious metals by natural amalgamation in the Las Cruces weathering profile (Iberian Pyrite Belt, SW Spain), Ore Geol. Rev. (2013), http://dx.doi.org/10.1016/j.oregeorev.2013.10.004

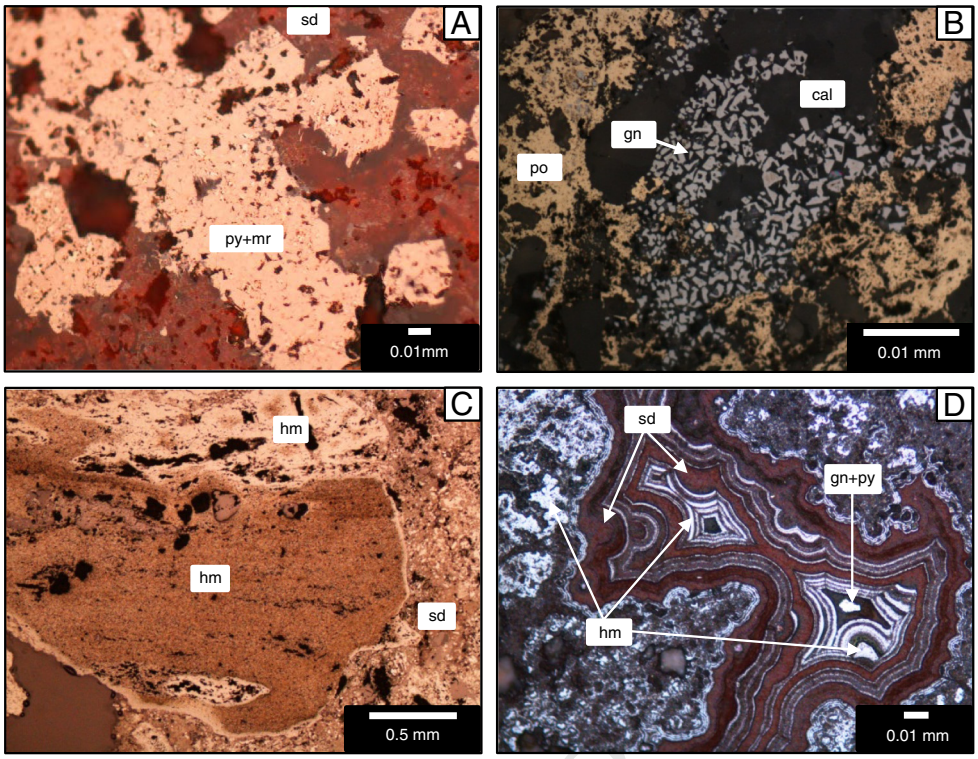

Fig. 5. Reflected light microscope images of the Las Cruces gossan. (A) intergrowth between massive siderite (sd) and subhedral aggregates of marcasite (mr) with pyrite (py) inclusions; (B) intergrowth between massive calcite (cal) and skeletal galena (gn) and pyrite (py); (C) relicts of massive hematite (hm) cemented by microcrystalline siderite (sd); and (D) microbands of alternating siderite (sd) and hematite (hem) and microcrystalline siderite filling voids.

Fig. 6 shows the Au–Ag–Hg ratio based on analytical data obtained using EPMA (Table 2). The Au–Ag–Hg system features two types of amalgams, described below.

Type 1 amalgam is rich in Au and Ag, with concentrations of up to 39.96 wt.% and 43.98 wt.%, respectively, and Hg values ranging between 23.23 wt.% and 28.95 wt.%. Two sub-groups can be differentiated depending on their chemical composition. The first one is richer in Au and poorer in Ag, with mean values of 39.09 wt.% and 32.49 wt.%, respectively, whereas the second one shows the opposite behavior, with mean Au and Ag concentrations of 25.95 wt.% and 43.04 wt.%, respectively (Fig. 7, Table 2). According to EPMA data and EDS-Scans, each of these sub-groups exhibits internal homogeneous composition. Amalgam type 1 mainly occurs in the carbonate-sulfide facies close to the contact with the cementation zone. Both sub-groups occur as skeletal, elongated grains of 1 to 50 μm in thickness associated with pyrite, sternbergite, and goethite, partially replaced by siderite (Fig. 6A, B).

Type 2 amalgam is rich in Ag and Hg, with small amounts of Au. The Ag values range between 21.42 wt.% and 49.53 wt.%, and the mean concentration of Hg is 60.30 wt.%. The Au concentration attains 2.28 wt.% (Fig. 7, Table 2). Two sub-groups can be identified based on Ag and Hg concentrations. One of them shows similar Ag and Hg values, with values around 45.57 wt.% and 49.66 wt.% respectively, whereas the other sub-group is richer in Hg and poorer in Ag, with mean values of 69.92 wt.% and 27.28 wt.%, respectively. No evidence of chemical zoning has been observed in type 2 amalgams. Both compositional sub-groups occur as grains (approximately 50 × 100 μm) filling elongated voids arranged parallel to the main foliation in the sheared black shales (Fig. 6C, D). Amalgam type 2 mainly occurs in the sheared black shale level. These appear as anhedral grains of approximately 50 × 100 μm, filling voids in the host rock. Sternbergite, miargyrite, Ag–Pb-sulfides, and sulfosalts are commonly associated with these Ag–Hg amalgams, all of which exhibit massive textures (Fig. 6E, F).

7. Discussion

7.1. Evolution of the Las Cruces gossan

The Las Cruces gossan lithology and mineralogy result from the complex redox history of the Las Cruces weathering profile, which can be explained as the result of the superposition of several genetic stages. During the Upper Oligocene–Lower Miocene exhumation of the IPB (Essalhi et al., 2011), the Las Cruces massive sulfide experienced oxidative weathering, gossan formation, and the precipitation of Fe-rich oxides, oxyhydroxides, and sulfates common in gossans (Fig. 5C). After the Neogene transgression, Las Cruces remained buried beneath the sedimentary cover. The interaction with meteoric fluids (Capitán, 2006), equilibrated with the carbonate-rich sedimentary pile above, resulted in physico-chemical changes towards reducing alkaline conditions (Capitán, 2006), favoring the formation of iron-reduced phases, such as carbonates and sulfides. As a result, early iron oxides, hydroxides, and sulfates were replaced by siderite and Fe-sulfides (Fig. 5A, D). These reducing conditions also involved the formation of galena and Pb-sulfosalts (Yesares et al., 2010) (Fig. 5B).

The Las Cruces gossan ore features provide strong evidence of the enrichment of immobile elements by the supergene lixiviation of massive sulfides (Blake, 2008). Thus, Au, Ag, and Hg were released from primary ores and are locally concentrated in the upper gossan by residual enrichment process. Amalgams were precipitated in the lower gossan during late stages to the supergene enrichment, as deduced from their textural relations with newly-formed phases and the kaolinitized host rock.

7.2. Relationship to other VMS deposits and weathering profiles in the region

Gossans in the IPB show typical features of massive sulfide weathering profiles (Capitán, 2006; Jambor et al., 2000; Scott et al.,

Please cite this article as: Yesares, L., et al., Supergene enrichment of precious metals by natural amalgamation in the Las Cruces weathering profile (Iberian Pyrite Belt, SW Spain), Ore Geol. Rev. (2013), http://dx.doi.org/10.1016/j.oregeorev.2013.10.004

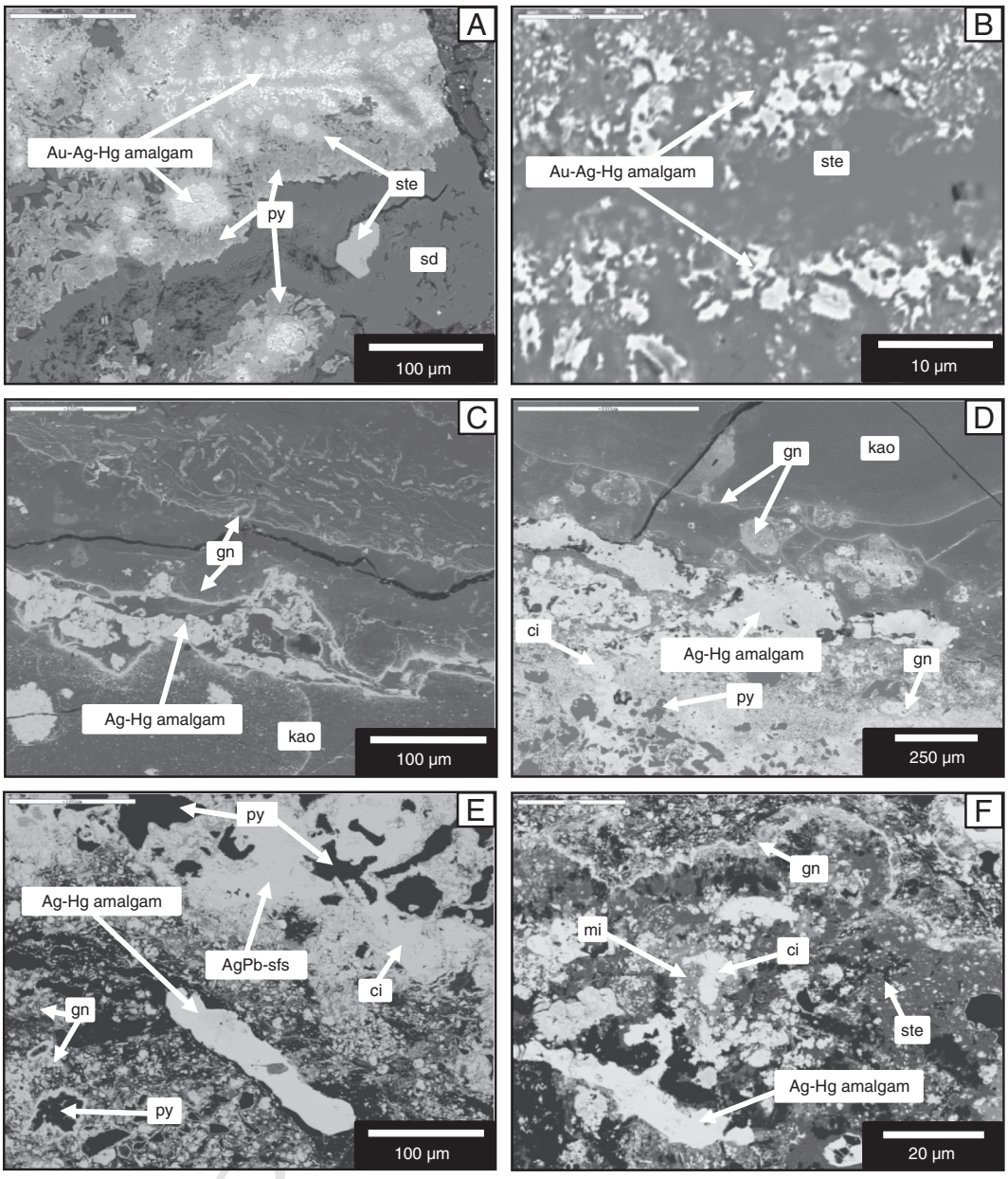

Fig. 6. Scanning electron microscope images of Las Cruces alloys. (A) Massive siderite (sd) with pyrite (py) and stembergite (ste) in siderite voids and skeletal crystal of Au–Ag–Hg amalgam; (B) skeletal Au–Ag–Hg amalgam; (C) kaolinitic (kao) matrix with massive galena in fine veins and late Ag–Hg amalgams filling voids; (D) kaolinitic (kao) matrix cementing pyrite, massive galena as cavity fillings, and late massive Ag–Hg amalgam; (E) massive Ag–Pb-sulfosalts (ssAgPb) cementing pyrite, equigranular aggregates of galena (gn) and massive cinnabar (ci), and Ag–Hg amalgam filling cavities; (F) massive stembergite (ste) and miargyrite (mi) cementing pyrite, fine veins of galena, and late massive cinnabar.

2001; Velasco et al., 2013) such as: (i) major mineralogy formed by oxidized facies such as goethite, hematite, minerals of the jarosite group, and quartz; (ii) the main textures include: massive, boxwork, colloform and open space fillings; and (iii) vertical zonation. IPB gossans exhibit three separate zones with gradual contact between them: a lower zone composed by goethite and quartz with jarosite, an intermediate zone comprised of goethite, quartz and hematite and an upper zone dominated by hematite and quartz (Velasco et al., 2013). The distribution of precious metals in the IPB gossans is highly variable showing maximum values of 10.5 ppm Au and 105 ppm Ag (Velasco et al., 2013). Precious metals occur as fine-grained particles of native Au and Ag, and as halides such as iodargyrite and chlorargyrite associated with minerals of the jarosite group (e.g. Capitán, 2006; Velasco et al., 2013). The Las Cruces gossan shows some analogies with IPB gossan profiles such as: (i) sharp contacts between gossans and massive sulfides (Velasco et al., 2013; Yesares et al., 2010); (ii) enrichment in lesser mobile elements by supergene lixiviation (Blake, 2008; Capitán, 2006); and (iii) precious metal content increasing close to the gossan-massive sulfide contact (Velasco et al., 2013). Nevertheless, there are important differences: (i) main mineralogy comprised of carbonates, Fe-sulfides and galena. Oxidized minerals such as Fe-oxyhydroxides and sulfates are scarcer; (ii) lack of vertical zonation; (iii) heterogeneity in precious metal distribution showing Au and Ag mean values of 5.1 ppm and 155 ppm respectively, and reaching maximum values up to 352 ppm Au and 18950 ppm Ag; and (iv) precious metals mainly occur as Au–Ag–Hg and Ag–Hg amalgam particles. Some of these peculiar features have also been described in the Lagoa Salgada weathering profile (Gaspar et al., 1993; Oliveira et al., 2011).

Exposed IPB supergene profiles were all developed under similar conditions, and being different in features they can show the result of their generation along several stages (Velasco et al., 2013). These involve Miocene exhumation of the massive sulfide bodies, the

Please cite this article as: Yesares, L., et al., Supergene enrichment of precious metals by natural amalgamation in the Las Cruces weathering profile (Iberian Pyrite Belt, SW Spain), Ore Geol. Rev. (2013), http://dx.doi.org/10.1016/j.oregeorev.2013.10.004

Table 2
EPMA analysis of neo-formed amalgams in the Las Cruces gossan. Basic statistic parameters (mean. maximum. minimum. and standard deviation) are shown.

Amalgam type	sample	Au	Hg	Ag	Total
Type 1	1-1	38.69	23.8	33.33	95.84
	1-2	39.44	23.59	32.6	95.63
	1-3	39.96	24.9	31.02	95.89
	1-4	39.16	23.36	33.35	95.89
	1-5	39.79	24.42	32.13	96.35
	1-6	38.13	23.23	34.1	95.47
	1-7	39.49	24.88	30.9	95.28
	1-8	38.03	23.8	32.47	94.3
	1-9	28.3	23.29	43.52	95.11
	1-10	26.23	27.32	41.74	95.29
	1-11	24.76	28.95	42.07	95.78
	1-12	26.32	25.98	43.28	95.58
	1-13	27.36	24.58	43.87	95.81
	1-14	24.98	26.96	43.98	95.92
	1-15	25.54	28.58	42.8	96.92
	1-16	25.48	27.23	43.25	95.96
	1-17	24.58	27.93	42.87	95.38
	Mean	32.13	25.46	38.08	95.67
	Max	39.96	28.95	43.98	96.92
	Min	24.58	23.23	30.90	94.30
	Std. dev.	6.83	1.98	5.51	0.56
Type 2	2-1	n.d.	49.82	46.94	96.76
	2-2	0.03	50.04	45.86	95.93
	2-3	0.02	49.24	46.7	95.96
	2-4	0.03	48.54	47.6	96.17
	2-5	n.d.	50.69	44.5	95.19
	2-6	n.d.	51	44.51	95.52
	2-7	0.01	52.91	46.18	99.12
	2-8	2.2	49.99	43.74	95.94
	2-9	2.28	50.82	42.09	95.19
	2-10	2.12	49.2	44.21	95.53
	2-11	1.88	50.96	42.58	95.42
	2-12	2.04	49.28	44.59	95.91
	2-13	2.13	48.67	44.32	95.12
	2-14	1.78	51.64	41.89	95.31
	2-15	n.d.	47.26	48.86	96.13
	2-16	0.03	47.35	48.03	95.42
	2-17	0.08	48.25	47.3	95.69
	2-18	n.d.	50.39	46.39	96.78
	2-19	n.d.	47.56	49.53	97.1
	2-20	0.036	73.77	21.99	95.79
	2-21	0.006	78.21	23.41	101.62
	2-22	n.d.	75.75	21.42	97.17
	2-23	n.d.	77.25	24.09	101.34
	2-24	0.011	73.57	22.37	95.95
	2-25	n.d.	74.9	22.85	97.75
	2-26	n.d.	75.35	23.96	99.31
	2-27	0.009	76.25	24.57	100.82
	2-28	n.d.	74.21	21.89	96.1
	2-29	n.d.	76.96	22.58	99.54
	2-30	n.d.	63.09	32.26	95.36
	2-31	n.d.	65.09	30.14	95.23
	2-32	0.076	64.42	31.42	95.93
	2-33	n.d.	64.46	31.45	95.92
	2-34	n.d.	63.25	34.12	97.37
	2-35	n.d.	64.46	30.55	95.01
	2-36	n.d.	65.6	30.75	96.36
	2-37	n.d.	65	30.92	95.93
	2-38	0.006	66.25	29.73	95.99
	2-39	n.d.	65.51	30.83	96.35
	2-40	n.d.	64.89	31.59	96.49
	Mean	0.37	60.30	35.97	96.64
	Max	2.28	78.21	49.53	101.62
	Min	0.00	47.26	21.42	95.01
	Std. dev.	0.79	11.08	9.89	1.72

n.d.: Not detected.

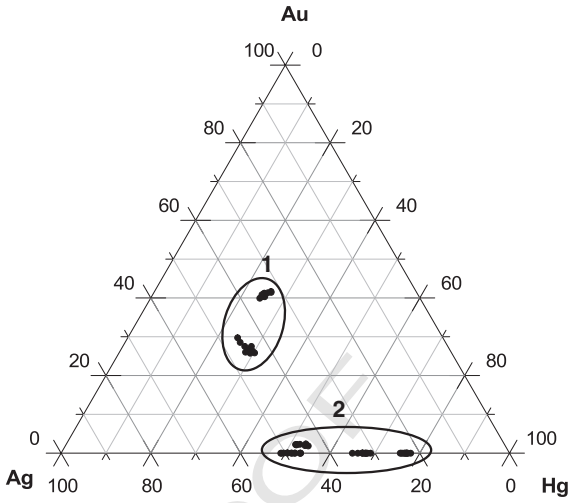

Fig. 7. Composition of amalgams in the Au–Ag–Hg ternary diagram. Two clusters can be distinguished according elemental ratios: Type 1 and Type 2.

subsequent oxidative weathering of sulfide minerals and a progressive intensification of the oxidation and leaching processes. Exposed IPB gossans have been subjected to subaerial conditions since the beginning of their formation to date, whereas Las Cruces and Lagoa Salgada gossans involve Miocene exhumation and massive sulfide oxidation followed by burial beneath the Tertiary cover and the evolution under the sedimentary pile. Examples of buried supergene profiles have been reported in VHMS deposits in the South Urals which are buried under Mesozoic–Cenozoic sediments. These supergene profiles are characterized by sideritized iron caps as well as newly-formed Fe-sulfides, galena, Hg-sulfides and Pb-sulfosalts (Belogub et al., 2003, 2008).

No exhaustive studies have been performed up to now about the source of the Las Cruces precious metals and Hg. Available geochemical data (Table 1), together with the lack of evidence of external supply, suggest the primary polymetallic and Cu-rich ores as the most feasible source for Au, Ag and Hg. In primary sulfides, Au is commonly closely associated with electrum (Hough et al., 2009), and As-rich pyrite or arsenopyrite (Cook and Chryssoulis, 1990; Reich et al., 2005; Sung et al., 2009), whereas tetrahedrite–tennantite is the most likely source of Ag (Sack, 1992) and Hg (Karup-Møller and Makovicky, 2003), with Ag-bearing galena (Boyle, 1979) and Hg-rich sphalerite also being common. In the IPB, precious metals in the massive sulfide ores occur as auriferous arsenopyrite, native Au and electrum associated with the polymetallic mineralization and the stockwork (Leistel et al., 1998). Examples of these precious metal-bearing IPB sulfides can be found in the La Zarza massive sulfides, where visible native Au, electrum and Au–Ag–Hg amalgams have been reported (Ruiz and Samper, 1995). In the Migollas deposit, Ag-rich tetrahedrite and bournonite, Hg-rich sphalerite and Au–Ag–Hg amalgams in massive sulfides have been described (Velasco et al., 1999). In Neves Corvo, Au-rich arsenopyrite, Ag-rich tetrahedrite, native Au and electrum are associated with Cu-rich sulfides and the stockwork zone (Pinto et al., 2005). In Lagoa Salgada, Ag-rich tetrahedrite has been reported in the primary sulfides (Gaspar et al., 1993). Finally, native Au and electrum occur in the Tharsis stockwork type mineralization (Leistel et al., 1998; Velasco et al., 2000).

Genetic models for precious metal mineralization in the IPB massive sulfide deposits include several stages. Velasco et al. (1999, 2000) suggested Au precipitation as nanoparticles within early pyrite, whereas Ag and Hg were suggested to have been included as solid solutions within the tetrahedrite and sphalerite crystal lattices. A later stage, during the massive sulfide genesis, involved the Au, Ag and Hg release from primary sulfides, transport at high temperature (200–350 °C) and precipitation of these elements as temperature decreased. Leistel et al. (1998) proposed two different mineralization processes, an earlier Au precipitation, as Au-rich electrum, at high temperature (300 °C) mainly associated to the stockwork zones, and a later Au formation stage as Ag–Hg-rich electrum and Au-rich arsenopyrite, at lower temperature (280 °C) and associated with polymetallic sulfides. Therefore, given the mineralogical and geochemical analogies between the Las

Table 3
Summary of main Au–Ag–Hg mineralization parameters used in the proposed genetic model for the Las Cruces deposit.

Gossan evolution stages	Environmental conditions and Au, Ag and Hg behavior	Neo-formed minerals	Au, Ag and Hg behavior and mineral equilibria	References
Stage I (Upper Oligocene–Lower Miocene) Tectonic uplifting, deposit exhumation and gossan formation	Oxygenated, acid-sulfate and chloride-rich conditions pH < 5.5; Eh > 0.9 V Precious metals are released from primary sulfides and enriched in the gossan	Fe-oxyhydroxides, Fe-sulfates, native Au, Ag-halides, Hg-sulfates	Suggested mobilization mechanism $4Au + 16Cl^- + 3O_2 + 12H^+ = 4AuCl_4^- + 6H_2O$ $4Ag + 4Cl^- + O_2 + 4H + = 4AgCl^0 + 2H_2O$ $Hg^{2+} + 2Cl^- + 3O_2 + 12H^+ = HgCl_2^0 + 6H_2O$ Suggested precipitation mechanism $4AuCl_4^- + 3Fe^{2+} + 6H_2O = Au^0 + 3Fe^{3+}OOH +$ $4Cl^- + 9H^+$ $AgCl^0 = AgCl$ $2HgCl_2^0 + 2Cl^- = Hg_2Cl_2 + Cl_2$ $HgCl_2^0 + H_2O = HgO + 2Cl^- + 2H^+$ $0.5Hg^{2+} + 3Fe^{3+} + 2SO_4^{2-} + 6H_2O =$ $Hg_{0.5}Fe_3(SO_4)_2(OH)_6 + 6H^+$	Mann (1984) Mann (1984) Saunders (1993) Dutrizac and Eno (1981)
Stage II (Upper Miocene Lower Pliocene) Ore burial under carbonate-rich sedimentary cover	Neutral and reduced conditions pH ~ 6–7; Eh < 0 V In the upper gossan: Buffered solutions and precious metal remobilization In the lower gossan: Migrating solutions interact with high reductant lithologies including organic matter-rich rocks	Siderite, calcite, Fe-sulfides, Pb-sulfides, Fe-oxyhydroxides, native Au, Hg, Ag-sulfates Fe-sulfides, Pb-sulfides, Ag-sulfides, cinnabar, amalgams	Suggested mobilization mechanism $2Au^0 + 4S_2O_3^{2-} + H^+ + 0.5O_2 = 2Au(SO_3)_2^{3-} + H_2O$ $2Ag^0 + 4S_2O_3^{2-} + H^+ + 0.5O_2 = 2Ag(SO_3)_2^{3-} + H_2O$ $Ag(SO_3)_2^{3-} + O_2 = Ag_2SO_4$ $Hg^{2+} + 0.5O_2 + H_2O = Hg(OH)_2^0$ $HgCl_2 + 2H_2O = Hg(OH)_2^0 + 2H^+ + Cl^-$ Suggested precipitation mechanism $Au(SO_3)_2^{3-} + O_2 = Au_2SO_4; Au_2SO_4 = 2Au^+ + SO_4^{2-}$ $Au^+ + Fe^{2+} + 2H_2O = Au^0 + FeO(OH) + 3H^+$ $Ag_2SO_4 + Fe^{3+} + H_2O = AgFe_3(SO_4)_2(OH)_6$ $Hg(OH)_2^0$ sorbed in oxides $Hg(OH)_2 + Fe^{2+} = Fe(OH)_3 + Hg^0$	Freyssinet (2005) Hepler and Olofsson (1975) Stroffregen (1986) Charlet et al. (2002)

Cruces primary ores and the main IPB massive sulfide deposits, they could be generalized to these IPB models for Las Cruces Au, Ag and Hg primary mineralization.

7.3. Las Cruces Au–Ag–Hg genetic model

In developing a model for the Las Cruces gossan Au–Ag–Hg mineralization, careful consideration must be given to the physico-chemical characteristics of the mineralizing solutions and data pertaining to the solubilities of Au, Ag, and Hg in a weathering profile. Thus, any model proposed for the Las Cruces gossan Au–Ag–Hg mineralization must accommodate the following features:

- The present mineralogical and geochemical features of the Las Cruces gossan are results of the overlapping of several genetic stages, including those related to oxidative weathering as well as those associated with changes in redox conditions during later burial beneath the Neogene sedimentary cover. This geological evolution involves hydrogeological flow fluctuations, oscillations of the water table, and changes in the physical and chemical characteristics of meteoric and basinal fluids. The environmental conditions at the gossan generation site changed progressively from oxidizing and acidic during the early gossan formation under surface exposure to near-neutral and reducing during the burial stage because of basinal fluid equilibration with the carbonate-rich sedimentary pile.
- An organic-matter-rich black shale horizon at the base of the gossan acts as a redox boundary suitable to Au–Ag–Hg precipitation.

With these features, a two-stage genetic model for Au–Ag–Hg amalgam formation is proposed (Table 3 and Fig. 8):

– Stage I: The presence of Fe-rich oxides and oxyhydroxides enclosed in later microcrystalline siderite (Fig. 5C) is a strong argument for the massive sulfide oxidation after its exhumation and weathering. This is also supported by the occurrence of gossan pebbles within the Neogene sedimentary cover (Fig. 3E) which indicates the weathering and oxidation of the massive sulfide. Under acidic pH, iron released from the sulfides is oxidized and precipitated as Fe-rich oxysulfate or oxyhydroxide (Bigham and Nordstrom, 2000). Thus, the gossan is enriched in Fe-bearing phases which can persist over a wide pH range, with goethite dominating at pH values of 3–6, but easily transformed to hematite upon dehydration (Thornber and Wildman, 1984).
Under these extreme conditions, precious metals and Hg are released from the primary sulfides and could be mobilized downward through the weathering profile as chloride complexes (Davis et al., 1997; Mann, 1984) according to Eqs. (1), (2), and (7) (see Section 2). The relationships between Au and limonite reported by Blake (2008) can be explained by the fixation of elemental Au associated to Fe-oxyhydroxide formation (Mann, 1984) (Eq. (3)), with Ag enriched as halides (Mann, 1984), whereas Hg could precipitate as halides, oxides, and sulfate minerals of the jarosite group (Dutrizac and Eno, 1981) through chemical reactions shown in Eqs. (10), (11), and (12), respectively.
– Stage II: The burial of the gossanized massive sulfides under the carbonate-rich sedimentary cover involved significant mineralogical and geochemical changes. Meteoric and basinal fluids were buffered to near-neutral conditions by interaction with the sedimentary pile, as is defined by the association of oxyhydroxides–siderite. According to textural criteria (i.e., microcrystalline siderite as cement of goethite and hematite fragments (Fig. 5C) or alternating microlayers of siderite and Fe-oxyhydroxide (Fig. 5D)), changes in chemical conditions occurred progressively to reach values of pH > 6.5 and Eh < 0 V, which are the siderite stability conditions (Garrels and Christ, 1965). During burial of the deposit and rising of the water table, the redox conditions were decreasingly reaching

Please cite this article as: Yesares, L., et al., Supergene enrichment of precious metals by natural amalgamation in the Las Cruces weathering profile (Iberian Pyrite Belt, SW Spain), Ore Geol. Rev. (2013), http://dx.doi.org/10.1016/j.oregeorev.2013.10.004

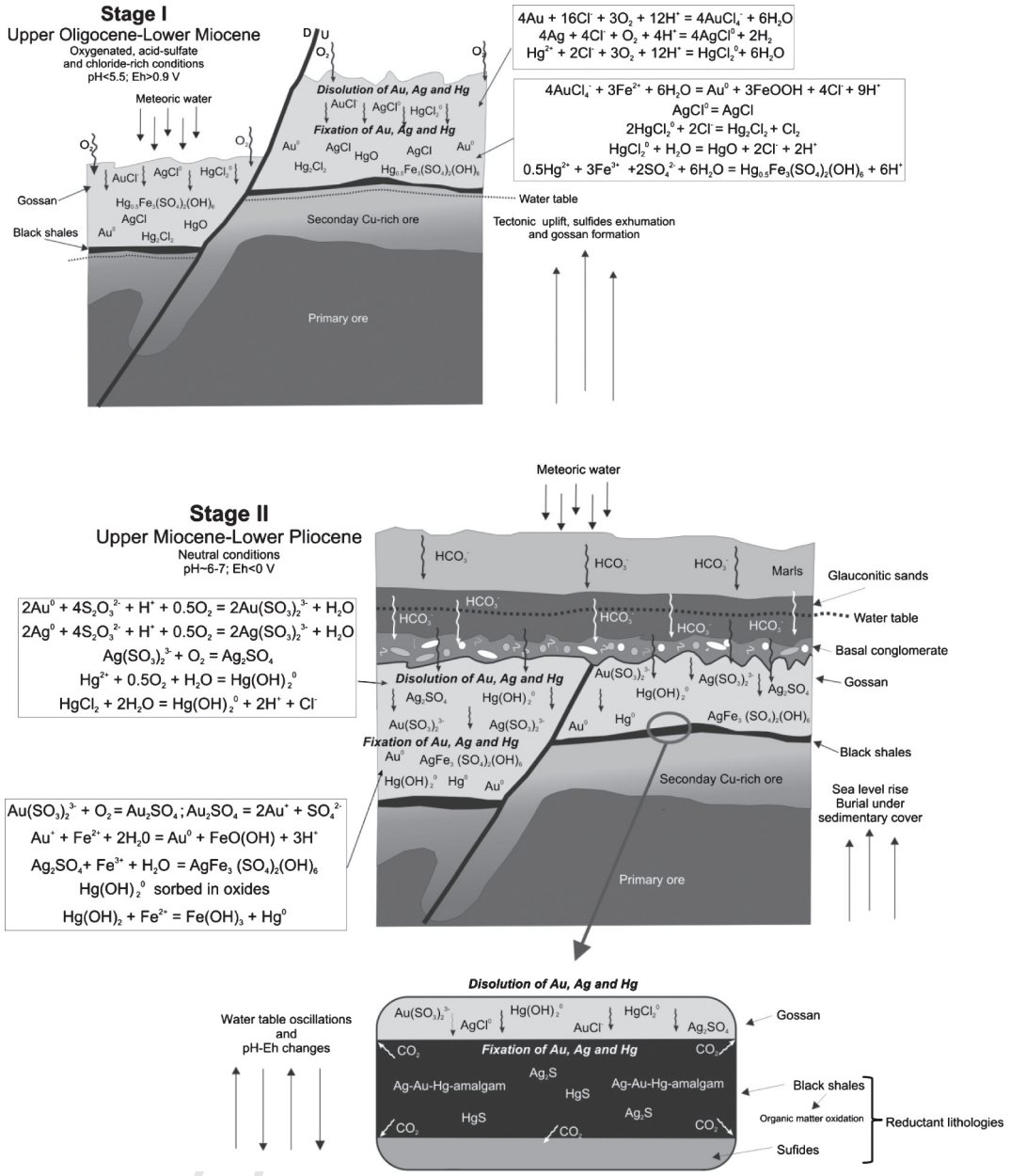

Fig. 8. Two-stage genetic model for the Las Cruces Au–Ag–Hg mineralization.

values of Eh < −0.3 V. This is suggested by the association of siderite–pyrite–pyrrhotite–galena (Garrels and Christ, 1965) (Fig. 5A, B). Hence, under these conditions, fluids migrated downward through the weathering profile producing remobilization of Hg, Ag, and Au as thiosulfate, sulfate, and hydroxide complexes (Benedetti and Bouleguè, 1991; Boyle, 1979; Freyssinet et al., 2005; Hepler and Olofsson, 1975; Webster and Mann, 1984) as shown in Eqs. (4), (5), (8), and (9). At this stage, the decomposition of Au, Ag, and Hg complexes involves the precipitation of Au and Hg by sorption during ferric hydroxide formation (Benedetti and Bouleguè, 1991; Davis et al., 1997; Freyssinet et al., 2005) through chemical reactions shown in Eqs. (6) and (13). These features can explain the native Au co-existence in sideritic and/or limonitic matrix described by Blake (2008). The Ag fixation seems to be associated with the precipitation of minerals of the jarosite group (Dutrizac and Jambor, 1987) if the conditions are acidic and oxygenated, while under reducing conditions Ag precipitated as sulfides as occur in the carbonate–sulfide facies.

After burial, the redox and pH changes in basinal fluids seem to be controlled by oscillations in the water table in view of mineralogical and textural features (Fig. 5A, B, D). The neo-formation of kaolinite and smectite can be regarded as evidence that oxidized meteoric fluids have circulated through the black shale resulting in the intense leaching of this lithology above the water table. In contrast, the mineralogical identifications of large amounts of newly-formed cinnabar and Ag-sulfides which are precipitated in Eh < 0 V conditions (Davis et al., 1996; Sato, 1992), are supported by the later lower gossan development under reducing conditions below the water table. Nevertheless, the black shale level seems to behave as an important redox barrier in such a way that it usually constitutes the limit between the gossanized and the cementation zone. These favored the partial remobilization of the metals to the lower part of the gossan.

The successive water table oscillations together with the changes in the pH–Eh conditions could produce several cycles of partial remobilization of Au, Ag, and Hg near the redox front and close to the sheared black shale level. The interaction of downward migrating fluids with

Please cite this article as: Yesares, L., et al., Supergene enrichment of precious metals by natural amalgamation in the Las Cruces weathering profile (Iberian Pyrite Belt, SW Spain), Ore Geol. Rev. (2013), http://dx.doi.org/10.1016/j.oregeorev.2013.10.004

highly reductant lithologies (i.e., black shales and massive sulfides) favors the precipitation of precious metals in elemental form. An analogous fixation mechanism of noble metals by fluid interactions with reduced lithologies has been reported for Au mineralizations in South Devon, England (Shepherd et al., 2005). In a similar way, the sheared black shale horizon, located at the boundary between the gossan and the sulfides, seems to play the primary role of the reductant front for Hg and precious metals in the Las Cruces deposit. The interactions of Au–Ag–Hg-rich solutions with the black shale level led to the oxidation and reduction of organic matter and sulfate respectively, together with the precipitation of Au, Ag, and Hg as native elements. This stage also involved the neo-formation of cinnabar, Ag-sulfides and sulfosalts as well as the precipitation of Au–Ag–Hg amalgams. Hence, the oxidizing processes linked to gossan formation appear to be efficient for the mobilization and enrichment of Au–Ag–Hg, whereas reducing processes associated with the decomposition and oxidation of organic matter are probably responsible for the deposition of Au–Ag–Hg amalgams in the Las Cruces gossan.

8. Concluding remarks

The geochemical and mineralogical features of the Las Cruces deposit show a high geochemical correlation between the Au, Ag, and Hg, which are highly concentrated near the base of the gossan, where the main mineral phases are Ag–Hg and Au–Ag–Hg alloys. These amalgams are mainly located in a strongly leached black shale horizon, which acted as an important redox front, in such a way that it usually constitutes the limit between the gossanized and primary sulfide ore.

Two ore-formation stages are identified. First, Au, Ag, and Hg were released by the dissolution of the primary sulfide ores under highly acidic and oxygenated conditions. These species were mobilized as chloride complexes and precipitated by reduction associated with Fe-oxyhydroxide formation and/or as halides and sulfates. Second, Au, Ag, and Hg were remobilized under neutral and slightly reduced conditions by the sediment-buffered solutions as thiosulfates, sulfates, and hydroxide complexes and their reprecipitation was linked to Au and Hg sorption during Fe-oxyhydroxide formation and Ag fixation as sulfates. Au, Ag, and Hg cyclic mobilizations, due to redox changes, generated metal-enriched solutions that precipitated after reaching the black shale horizon located at the base of the gossan, which act as a redox boundary due to the organic matter consumption during the supergene processes. This stage featured Au, Ag, and Hg reduction, resulting in the neo-formation of amalgams, cinnabar, and Ag-sulfides. These amalgams are the main Au–Ag-bearing mineral phases in the Las Cruces gossan and provide a possible additional economic resource for the deposit.

This report is the first characterization of precious metal secondary enrichment by natural amalgamation of Au–Ag–Hg under supergene conditions. The mechanism involved in these precious metal enrichments differs from those proposed in the classic genetic model for supergene precious metal ores.

References

Almodóvar, G.R., Sáez, R., Pons, J.M., Maestre, A., Toscano, M., Pascual, E., 1998. Geology and genesis of the Aznalcollar massive sulphide deposits, Iberian Pyrite Belt, Spain. Miner. Deposita 33, 111–136.

Aylmore, M.G., Muir, D.M., 2001. Thiosulfate leaching of gold—a review. Miner. Eng. 14, 135–174.

Barrie, C.T., 2002. U–Pb geochronology of VMS mineralization in the Iberian Pyrite Belt. Miner. Deposita 37, 684–703.

Belogub, E., Novoselov, C., Spiro, B., Yakovleva, B., 2003. Mineralogical and sulphur isotopic features of the supergene profile of Zapadno–Ozernoye massive sulphide and gold-bearing gossan deposit, South Urals. Mineral. Mag. 67, 339–354.

Belogub, E.V., Novoselov, K.A., Yakovleva, V.A., Spiro, B., 2008. Supergene sulphides and related minerals in the supergene profiles of VHMS deposits from the South Urals. Ore Geol. Rev. 33, 239–254.

Benedetti, M., Bouleguè, J., 1991. Mechanism of Au transfer and deposition in a supergene environment. Geochim. Cosmochim. Acta 55, 1539–1547.

Bigham, J.M., Nordstrom, D.K., 2000. Iron and aluminum hydroxysulfates from acid sulfate waters, in sulfate minerals: crystallography, geochemistry & environmental significance. In: Alpers, C.N., Jambor, J.L., Nordstrom, D.K. (Eds.), Rev. Mineral. Geochem., 40, pp. 303–350.

Blake, C., 2008. The mineralogical characterisation and interpretation of a precious metal-bearing fossil gossan, Las Cruces, Spain: Unpublished PhD Thesis. Cardiff: University of Wales.

Boyle, R.W., 1979. The geochemistry of Au and its deposits. Bull. Geol. Surv. Can. 280, 1–584.

Boyle, R.W., Alexander, W.M., Ashin, G.E.M., 1975. Some observations on the solubility of Au. Bull. Geol. Surv. Can. 75–24.

Capitán, M.A., 2006. Mineralogía y geoquímica de la alteración superficial de depósitos de sulfuros masivos en la Faja Pirítica Ibérica: Unpublished PhD Thesis. University of Huelva, Spain.

Capitán, M.A., Nieto, J.M., Sáez, R., Almodóvar, G.R., 2003. Caracterización textural y mineralógica del gossan de Filón Sur (Tharsis, Huelva). Boll. Soc. Esp. Mineral. 26, 45–58.

Carvalho, D., 1976. Consideraçoes sobre o vulcanismo da regiao de Cercal-Odemira. Suas relaçoes com a Faixa Piritosa. Comun. Serv. Geol. Port. 60, 215–238.

Charlet, L., Bosbach, D., Peretyashko, T., 2002. Natural attenuation of TCE, As, Hg linked to the heterogeneous oxidation of Fe (II): an AFM study. Chem. Geol. 190, 303–319.

Cook, N.J., Chryssoulis, S.L., 1990. Concentrations of "Invisible Au" in the common sulfides. Can. Mineral. 28, 1–16.

Davis, A., Bloom, N.S., Shane, S., Hee, Q., 1997. The environmental geochemistry and bioaccessibility of Hg in soils and sediments. Risk Anal. 17, 557–569.

Dutrizac, J.E., Eno, T.T., 1981. The synthesis of Hg jarosite and the Hg concentration in jarosite family minerals. Can. Mineral. 19, 559–569.

Dutrizac, J.E., Jambor, J.L., 1987. Behaviour of Ag during jarosite precipitation. Trans. Inst. Min. Metall. 80, 206–218.

Essalhi, M., Sizaret, S., Barbanson, L., Chen, Y., Lagroix, F., Demory, F., Nieto, J.M., Sáez, R., Capitán, M.A., 2011. A case study of the internal structures of gossans and weathering processes in the Iberian Pyrite Belt using magnetic fabrics and paleomagnetic dating. Miner. Deposita 46, 981–999.

Freyssinet, P., Butt, C.R.M., Morris, R.C., Piantone, P., 2005. Ore-forming processes related to lateritic weathering. In: Hedenquist, J.W., Thomson, J.F.H., Goldfarb, R.J., Richards, J.P. (Eds.), Economic Geology 100th Anniversary Volume. Economic Geology, pp. 681–722.

Garrels, R.M., Christ, C.L., 1965. In: Harper, Row (Eds.), Solutions, Minerals and Equilibria.

Gaspar, O.C., Oliveira, V.M.J., Matos, J.M.X., 1993. Nota preliminar sobre os sulfuretos macicos da Jazida da Lagoa Salgada, Faixa Piritosa Ibérica, Portugal: 11° Congr. Geoquímica. Mem. Lab. Min. Geol. 3, 239–242.

González, F., Moreno, C., Sáez, R., Clayton, G., 2002. Ore Genesis age of the Tharsis Mining District (Iberian Pyrite Belt): a palynological approach. J. Geol. Soc. London 159, 229–232.

González, F., Moreno, C., Santos, A., 2006. The massive sulfide event in the Iberian Pyrite Belt: confirmatory evidence from the Sotiel–Coronada. Geol. Mag. 143, 821–827.

Gray, D.J., Butt, C.R.M., Lawrance, L.M., 1992. The geochemistry of gold in lateritic terrains. In: Butt, C.R.M., Zeegers, H. (Eds.), Regolith Exploration Geochemistry in Tropical and Subtropical Terrains. Handbook of Exploration Geochemistry, 4, pp. 461–482.

Groen, J.C., Craig, J.R., Rimstidt, J.D., 1990. Au-rich rim formation on electrum grains in placers. Can. Mineral. 28, 207–228.

Hepler, L.G., Olofsson, G., 1975. Hg-thermodynamic properties, chemical-equilibria, and standard potentials. Chem. Rev. 75, 585–602.

Hough, R., Noble, R., Hitchen, G., Hart, G., Reddy, S., Saunders, M., Clode, P., Vaughan, D., Lowe, J., Gray, D., Butt, C.R., Verrall, M., 2008. Naturally occurring gold nanoparticles and nanoplates. Geology 36, 571–574.

Hough, R.M., Butt, C.R.M., Buhner, J.F., 2009. The mineralogy, crystallography and metallography of gold. Elements 5, 297–302.

Jambor, J.L., Nordstrom, D.K., Alpers, C.N., 2000. Metal-sulfate salts from sulphide mineral oxidation, in sulfate minerals: crystallography, geochemistry & environmental signifícance. In: Alpers, C.N., Jambor, J.L., Nordstrom, D.K. (Eds.), Rev. Mineral. Geochem., 40, pp. 303–350.

Julivert, T.M., Fontboté, J.M., Ribeiro, A., Conde, L., 1974. Mapa tectónico de la Península Ibérica y Baleares. Escala 1:1,000,000. Ins. Geol. Min. Esp.

Karup-Møller, S., Makovicky, E., 2003. Exploratory studies on element substitutions in synthetic tetrahedrite. Part V. Mercurian tetrahedrite. Neues Jb. Mineral. 179, 73–83.

Knigth, F., 2000. The mineralogy, geochemistry and genesis of the secondary sulphide mineralization of the Las Cruces Deposit, Spain: Unpublished PhD Thesis. Cardiff: University of Wales.

Krupp, R.E., Weiser, T., 1992. On the stability of Au–Ag alloys in the weathering environment. Miner. Deposita 27, 268–275.

Leistel, J.M., Marcoux, E., Thiéblemont, D., Quesada, C., Sánchez, A., Almodóvar, G.R., Pascual, E., Sáez, R., 1998. The volcanic-hosted massive sulfide deposits of the Iberian Pyrite Belt. Review and preface to the thematic issue. Miner. Deposita 33, 2–30.

Mann, A.W., 1984. Mobility of Au and Ag in lateritic weathering profiles: some observations from Western Australia. Econ. Geol. 79, 38–50.

Marcoux, E., Moelo, Y., Leistel, J.M., 1996. Compared ore mineralogy and geochemistry of the massive sulfide and stringer ore deposits of the Southern Spain. Miner. Deposita 31, 1–26.

Moreno, C., Capitán, M.A., Doyle, M., Nieto, J.M., Ruiz, F., Sáez, R., 2002. Edad mínima del gossan de Las Cruces: implicaciones sobre el inicio de los ecosistemas extremos en la Faja Pirítica Ibérica. Geogaceta 33, 67–70.

Nesbit, R.W., Pascual, E., Fanning, C.M., Toscano, M., Sáez, R., Almodóvar, G.R., 1999. U–Pb dating of stockwork zircons from the Eastern Iberian Pyrite Belt. J. Geol. Soc. London 156, 7–10.

Nieto, J.M., Almodóvar, G.R., Pascual, E., Sáez, R., Jagoutz, E., 2000. Evidencias isotópicas sobre el origen de los metales en los sulfuros masivos de la Faja Pirítica Ibérica. Cad. Lab. Xeol. Laxe 25, 139–142.

Please cite this article as: Yesares, L., et al., Supergene enrichment of precious metals by natural amalgamation in the Las Cruces weathering profile (Iberian Pyrite Belt, SW Spain), Ore Geol. Rev. (2013), http://dx.doi.org/10.1016/j.oregeorev.2013.10.004

Nocete, F., Álex, E., Nieto, J.M., Sáez, R., Bayona, M.R., 2005. An archaeological approach to regional environmental pollution in the South-Western Iberian Peninsula related to Third Millennium BC mining and metallurgy. J. Archaeol. Sci. 32, 1566–1576.

Oliveira, D.P.S., Matos, J.X.M., Rosa, C.J.P., Rosa, D.R.N., Figueiredo, M.O., Silva, T.P., Guimarães, F., Carvalho, J.R.S., Pinto, Á.M.M., Relvas, J.R.M.S., Reiser, F.K.M., 2011. The Lagoa Salgada orebody, Iberian Pyrite Belt, Portugal. Econ. Geol. 106, 1111–1128.

Pinto, A.M.M., Relvas, F.J.M.R.S., Barriga, J.A.S., Munha, J., Pacheco, N., Scott, S.D., 2005. Gold mineralization in recent and ancient volcanic-hosted massive sulfides. The PACMANUS field and the Neves Corvo deposit: Mineral Deposit Research: Meeting the Global Challenge.1 and 2, pp. 683–686.

Reich, M., Kesler, S.E., Utsunomiya, S., Palenik, C.S., Chryssoulis, S., Ewing, R.C., 2005. Solubility of gold in arsenian pyrite. Geochim. Cosmochim. Acta 69, 2781–2796.

Relvas, J.M.R.S., Barriga, F.J.A.S., Pinto, A., Ferreira, A., Pacheco, N., Barriga, G., Baptista, D., Oliveira, V., Munhá, J., Hutchinson, R.W., 2002. The Neves Corvo deposit, Iberian Pyrite Belt, Portugal: impact and future, 25 years after the discovery. Soc. Econ. Geol. Spec. Publ. 9, 155–176.

Rolla, E., Chakrabarti, C.L., 1982. Kinetics of decomposition of tetrathionate, trithionate and thiosulphate in alkaline media. Environ. Sci. Technol. 16, 852–857.

Ross, A.M., 1997. Supergene Au enrichment of the Precambrian aged Flambeau gossan, Flambeau Mine, Rusk County, Wisconsin: Unpublished PhD Thesis. University of Utah.

Ruiz, C., Samper, J., 1995. Presencia de amalgama Au–Ag–Hg en el Cinturon Piritico Iberico. Geogaceta 18, 184–186.

Sack, R.O., 1992. Thermochemistry of tetrahedrite–tennantite fahlores. In: Ross, N.L., Price, G.D. (Eds.), The Stability of Minerals. Chapman and Hall, pp. 243–266.

Sáez, R., Pascual, E., Toscano, M., Almodóvar, G.R., 1999. The Iberian type of volcano-sedimentary massive sulfide deposits. Miner. Deposita 34, 549–570.

Sáez, R., Nocete, F., Nieto, J.M., Capitán, M.A., Rovira, S., 2003. The extractive metallurgy of copper from Cabezo Juré, Huelva, Spain: chemical and mineralogical study of slags dated to the Third Millenium B.C. Can. Mineral. 41, 627–638.

Sáez, R., Moreno, C., González, F., 2008. Synchronous deposition of massive sulfide deposits in the Iberian Pyrite Belt: new data from Las Herrerías and La Torerera ore-bodies. Compt. Rendus Geosci. 340, 829–839.

Sato, M., 1992. Persistency-field Eh-pH diagrams for sulfides and their application to supergene oxidation and enrichment of sulfide ore bodies. Geochim. Cosmochim. Acta 56, 3133–3156.

Saunders, J.A., 1993. Supergene oxidation of bonanza Au–Ag veins at the Sleeper Deposit, Nevada, USA: implications for hydrochemical exploration in the Great Basin. J. Geochem. Explor. 47, 359–375.

Schermerhorn, L.J.G., 1971. An outline stratigraphy of the Iberian Pyrite Belt. Bol. Geol. Min. 82, 239–268.

Scott, K.M., Ashley, P.M., Lawie, D.C., 2001. The geochemistry, mineralogy and maturity of gossans derived from volcanogenic Zn–Pb–Cu deposits of the eastern Lachlan Fold Belt, NSW, Australia. J. Geochem. Explor. 72, 169–191.

Shepherd, T.J., Bouch, J.E., Andrew, G.G., McKervey, J.A., Naden, J., Scrivener, R.C., Styles, M.T., Large, D.E., 2005. Permo-Triassic unconformity-related Au–Pd mineralization, South Devon, UK: new insights and the European perspective. Miner. Deposita 40, 24–44.

Silva, J.B., Oliveira, J.T., Ribeiro, A., 1990. South Portuguese zone. Structural outline. In: Dallmeyer, R.D., Martinez Garcia, E. (Eds.), Pre-Mesozoic Geology of Iberia. Springer-Verlag, Berlin, pp. 348–362.

Simancas, J.F., 1983. Geología de la extremidad oriental de la Zona Surportuguesa: Unpublished PhD Thesis. University of Granada, Spain.

Stroffregen, R., 1986. Observations on the behaviour of Au during supergene oxidation at Summitville, Colorado, USA and implications for electrum stability in the weathering environment. Appl. Geochem. 2, 549–558.

Sung, Y.H., Brugger, J., Ciobanu, L., Pring, A., Skinner, W., Nugus, M., 2009. Invisible Au in arsenian pyrite and arsenopyrite from a multistage Archaean Au deposit: Sunrise Dam, Eastern Au fields Province, Western Australia. Miner. Deposita 44, 765–791.

Thornber, M.R., Wildman, J.E., 1984. Supergene alteration of sulphides, VI. The binding of Cu, Ni, Zn, Co and Pb with iron-bearing gossan minerals. Chem. Geol. 44, 399–434.

Tornos, F., González Clavijo, E., Spiro, B., 1998. The Filón Norte orebody (Tharsis, Iberian Pyrite Belt): a proximal low-temperature shale-hosted massive sulphide in a thin-skinned tectonic belt. Miner. Deposita 33, 150–169.

Velasco, F., Yanguas, A., Sánchez-España, J., Yusta, I., Herrero, J.M., Santos, A., Prada, J.M., 1999. In: Stanley, C.J. (Ed.), A Hg-rich Gold Mineral Association in the Migollas Massive Sulfide Deposit from the IPB, Spain, 2. Balkema, pp. 609–612.

Velasco, F., Sánchez-España, J., Yanguas, A., Tornos, F., 2000. The occurrence of gold in the sulfide deposits of the Iberian Pyrite belt: evidence of precious metal remobilization. In: Gemmell, Pongratz (Eds.), CODES, pp. 221–223.

Velasco, F., Herrero, J.M., Suárez, S., Yusta, I., Alvaro, A., Tornos, T., 2013. Supergene features and evolution of gossans capping massive sulphide deposits in the Iberian Pyrite Belt. Ore Geol. Rev. 53, 181–203.

Viñals, J., Roca, A., Cruells, M., Nuñez, C., 1995. Characterisation and cyanidation of Rio Tinto Gossan ores. Can. Metall. Q. 34, 115–122.

Vlassopoulos, D., Wood, S.A., 1990. Gold speciation in natural waters: I. Solubility and hydrolysis of gold in aqueous solution. Geochim. Cosmochim. Acta 54, 3–12.

Webster, J.G., 1986. The solubility of Au and Ag in the system Au–Ag–S–O_2–H_2O at 25 °C and 1 atm. Geochim. Cosmochim. Acta 50, 245–255.

Webster, J.G., Mann, A.W., 1984. The influence of climate, geomorphology and primary geology on the supergene migration of Au and Ag. J. Geochem. Explor. 22, 21–42.

Wood, S.A., 1990. The interaction of dissolved platinum with fulvic acid and simple organic acid analogues in aqueous solutions. Can. Mineral. 20, 665–674.

Yesares, L., Nieto, J.M., Sáez, R., Almodóvar, G.R., Videira, J.C., 2010. El gossan de Las Cruces (FPI): Litología y evolución mineralógica. Macla 13, 225–226.

Yesares, L., Sáez, R., Nieto, J.M., Almodóvar, G., 2012. Mineralogía del Enriquecimiento Secundario de Cu del Yacimiento Las Cruces, Sevilla. Macla 16, 226–227.

Yesares, L., Sáez, R., Nieto, J.M., Almodóvar, G., 2013n. The Las Cruces Orebody, Iberian Pyrite Belt, Spain (in preparation). Q22

Please cite this article as: Yesares, L., et al., Supergene enrichment of precious metals by natural amalgamation in the Las Cruces weathering profile (Iberian Pyrite Belt, SW Spain), Ore Geol. Rev. (2013), http://dx.doi.org/10.1016/j.oregeorev.2013.10.004